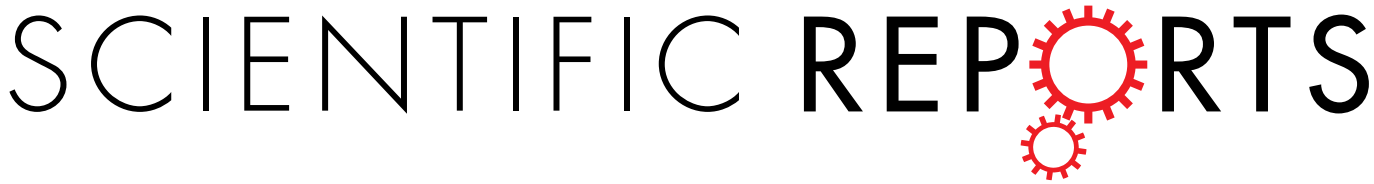

OPEN

Received: 10 April 2015
Accepted: 20 October 2015
Published: 26 November 2015

Trends of pH decrease in the Mediterranean Sea through high frequency observational data: indication of ocean acidification in the basin

Susana Flecha[1], Fiz F. Pérez[2], Jesús García-Lafuente[3], Simone Sammartino[3], Aida. F. Ríos[2] & I. Emma Huertas[1]

A significant fraction of anthropogenic carbon dioxide (CO_2) released to the atmosphere is absorbed by the oceans, leading to a range of chemical changes and causing ocean acidification (OA). Assessing the impact of OA on marine ecosystems requires the accurate detection of the rate of seawater pH change. This work reports the results of nearly 3 years of continuous pH measurements in the Mediterranean Sea at the Strait of Gibraltar GIFT time series station. We document a remarkable decreasing annual trend of -0.0044 ± 0.00006 in the Mediterranean pH, which can be interpreted as an indicator of acidification in the basin based on high frequency records. Modeling pH data of the Mediterranean outflow allowed to discriminate between the pH values of its two main constituent water masses, the Levantine Intermediate Water (LIW) and the Western Mediterranean Deep Water (WMDW). Both water masses also exhibited a decline in pH with time, particularly the WMDW, which can be related to their different biogeochemical nature and processes occurring during transit time from formation sites to the Strait of Gibraltar.

CO_2 emissions from fossil fuels burning and land use change since the industrial revolution have caused a considerable increase in atmospheric CO_2 concentrations[1]. Recent investigations have estimated that cumulative emissions of CO_2 have reached in the period from 1870 to 2013 about 535 ± 55 GtC[2]. However, a significant CO_2 amount has been captured from the atmosphere by natural sinks, such as the terrestrial biosphere and the ocean. In particular, the global oceans have absorbed about 30% of the anthropogenic carbon emissions over the past 200 years[3].

The withdrawal of CO_2 by the oceans has, however, drastic consequences for the marine environment, as it originates a rise in average surface ocean concentration of H^+ that leads to a pH decrease in seawater and a range of chemical changes known collectively as "the other CO_2 problem" or the ocean acidification (OA) phenomenon[4,5]. The impact of OA on marine biogeochemical cycles and biota has been well documented by laboratory studies and already observed to occur in certain ocean areas[6–9]. It has been suggested that the Mediterranean Sea (MS) represents one of the world's most sensitive ocean regions to increasing atmospheric CO_2 and the subsequent OA[10,11]. Nevertheless, contradicting observations of pH changes with time have been reported in the basin. A recent study affirms that the MS is already acidified,

[1]Instituto de Ciencias Marinas de Andalucía, (CSIC), Polígono Río San Pedro, s/n, 11519, Puerto Real, Cádiz, Spain. [2]Instituto de Investigaciones Marinas, (CSIC), Eduardo Cabello, 6, 36208, Vigo, Spain. [3]Physical Oceanography Group, University of Málaga, Campus de Teatinos s/n, 29071, Málaga, Spain. Correspondence and requests for materials should be addressed to S.F. (email: susana.flecha@icman.csic.es) or I.E.H. (email: emma.huertas@icman.csic.es)

although distinct OA rates are provided depending on the degree of anthropogenic carbon accumulation by a particular sub-basin, with regional pH decreases oscillating between −0.055 to −0.156 pH units with respect to the preindustrial levels[12]. On the other hand, another work points out to pH reductions between 0.005 to 0.06 pH units due to the anthropogenic carbon storage in the basin during the same period[13]. Moreover, it has been proposed that the pH decline would be amplified in the MS due to its higher capacity for CO_2 absorption in relation to open ocean regions[14,15] and the relatively short ventilation times of its water masses[14], statements that were challenged recently by a modelling approach[13] which indicates that the average anthropogenic change in surface pH does not differ significantly from the global-ocean average.

Considerable efforts have been made over the last decade to characterize the carbonate system in Mediterranean water masses[16–18], to explore how much anthropogenic CO_2 has been taken up by this semi-enclosed sea and to assess the corresponding pH diminution[13,14,19,20]. Most of these studies rely on discrete data sets that extend over a specific period of time or cover a particular Mediterranean sub-region. Thus, sometimes, these studies lead to discrepant conclusions when comparisons between data acquired in different periods, using distinct techniques and/or in distant locations are made.

The assessment of the marine ecosystems responses to the oceanic CO_2 uptake requires then sustained observations that provide the needed high frequency data about changes in ocean chemistry. At present, this type of measurements is being collected in a few ocean time-series[21]. The continuous monitoring of the carbon system parameters (and other tracers for hydrography and biochemistry) in these key sites have supplied relevant information on the ocean CO_2 sink and the derived pH changes in different regions, confirming a general OA trend over the past two decades.

Sustained time-series observations also started in the Strait of Gibraltar (SG) a decade ago through the establishment of the GIFT (Gibraltar Fixed Time Series) observatory, since this region represents a privileged site to observe the evolution of the Mediterranean waters over time. This narrow channel (14 km wide in its narrowest section) is the only connection of the MS with the North Atlantic, thereby playing a major role in the global circulation and biogeochemistry of the basin[22,23].

The circulation pattern in the SG has been traditionally described as a two-layer system, with surface Atlantic water (AW) flowing eastwards to the MS and the Mediterranean Outflow Water (MOW) moving westward to the Atlantic Ocean underneath. The AW enters the MS and flows clockwise in the Alboran Sea (AS, Fig. S1). Subsequent surface circulation patterns at the basin level are influenced by deep and intermediate water formation driven by strong winds, which is in turn affected and amplified by topography. Deep and intermediate waters are formed in four major areas: the Levantine Basin (LB, Fig. S1), the source of the Levantine Intermediate Water (LIW); the Gulf of Lions (GL, Fig. S1) where the Western Mediterranean Deep Water (WMDW) is formed; and two adjacent regions, the Adriatic and the Aegean Seas (AdS, AeS, respectively in Fig. S1), which together merge to form the Eastern Mediterranean Deep Water (EMDW). The MOW that leaves the basin through the Strait of Gibraltar is then a mixture of these intermediate and deep waters, fundamentally LIW, which flows across the Strait of Sicily (SS, Fig. S1) into the Western Mediterranean basin, and the WMDW, which occupies the bottom layer[24]. The contribution of the AW that penetrates into the MS in surface to the final outflow exiting the basin is negligible[25]. By monitoring the hydrography and biogeochemistry of the MOW in the SG, the history and evolution of the main intermediate and deep Mediterranean water masses can be examined.

The exchange of waters of different ages carrying diverse concentrations of biogeochemical properties in the SG also influences global inventories in the two neighbour regions[26,27]. Regarding the marine carbon cycle, a net transport of anthropogenic carbon from the Atlantic towards the Mediterranean has been identified[19,20,26], which has been indeed responsible for 25% of the basin-wide CO_2 uptake over the last 200 years[13].

In this work, we use pH measurements taken at the GIFT at a high sampling rate to assess temporal trends of pH change in Mediterranean waters. Data were obtained by autonomous sensors installed in a mooring line deployed at the Espartel Sill (ES, Fig. S1), which has been proven to be the most suitable section in the SG for monitoring the MOW[20,24,25,27–29]. Results presented here correspond to the first continuous pH records at a high temporal resolution registered in the channel from August 2012 to June 2015. Our work provides the first rates of pH decrease in the MOW and in its forming water masses separately, which can be considered indicators of OA in the basin, confirming previous evidence[12,13,15]. In addition, by using a simple model, we present a tool for tracking pH and its temporal variability in the MS.

Results and Discussion

Water masses and pH. From August 2012 to June 2015, the data collected at the mooring site fluctuated within small ranges of values. Potential temperature (Θ) oscillated from 13.01 to 13.63 °C, salinity from 38.01 to 38.48 and pH in total scale at a reference temperature of 25 °C (pH_{T25}) from 7.8618 to 7.9370 (Fig. 1). The pH_{T25} mean value was 7.8934 ± 0.0076 ($n = 15937$), which is in good agreement with the average pH in the MOW obtained from sustained spectrophotometric pH_{T25} measurements taken periodically within this layer at the GIFT stations from 2005 to 2014 ($n = 102$) and equivalent to 7.8875 ± 0.0124.

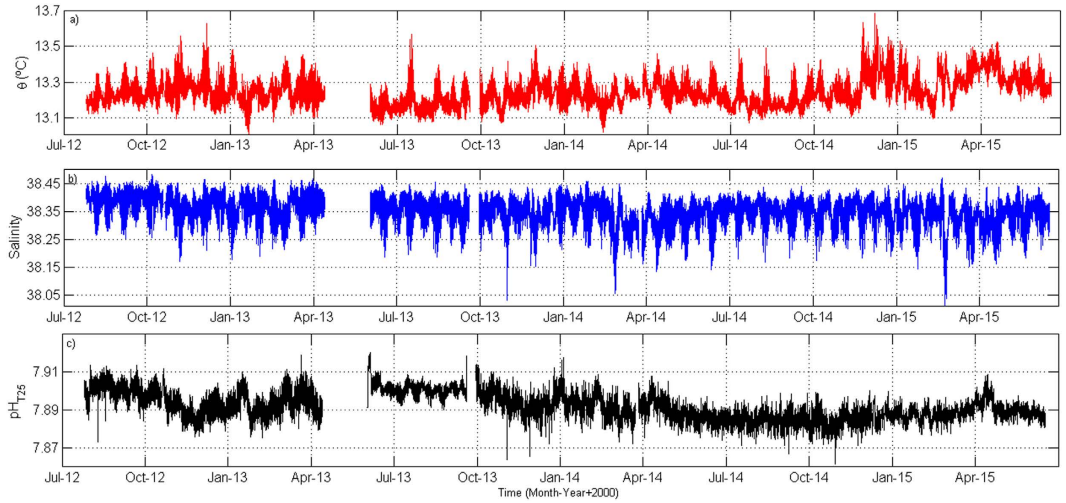

Figure 1. (**a**) Potential temperature (Θ), (**b**) Salinity obtained with the CT and (**c**) SAMI-pH data from August 2012 to June 2015.

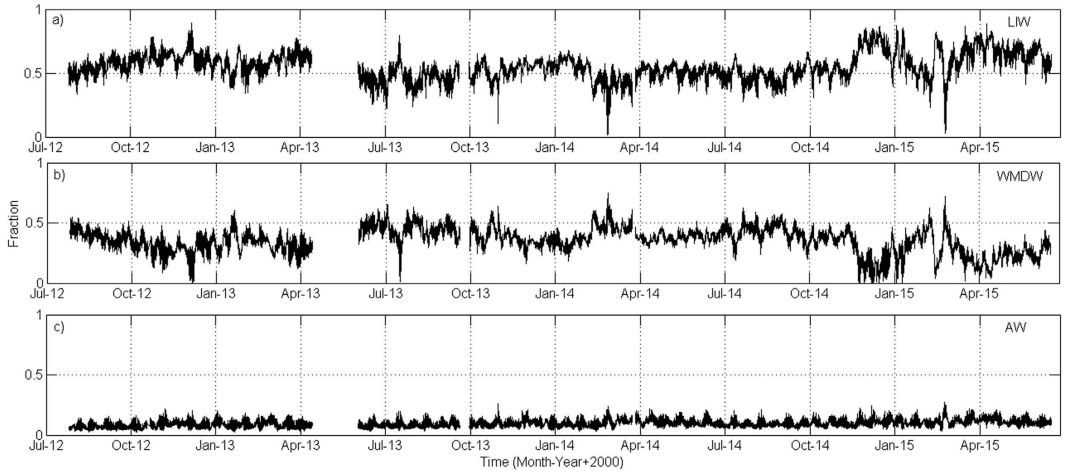

Figure 2. Fractions of the water masses forming the MOW during the monitoring period, according to the OMP analysis (see text): (**a**) LIW, (**b**) WDMW and (**c**) AW.

Water masses fractions variability in the MOW, discriminated with an OMP (Optimum MultiParameter) analysis[30], (see *SI text* for more details), clearly describes seasonal and interannual fluctuations (Fig. 2). During the monitoring period, the LIW appeared to dominate the outflow most of the time, with a mean fraction of 0.55 ± 0.1 (Fig. 2a) whereas the WMDW showed a fraction of 0.36 ± 0.1 (Fig. 2b). Because of the sampling depth, the presence of the AW (Fig. 2c) was almost negligible within the MOW, with an average fraction of 0.09 ± 0.03, confirming historic observations[25].

As previously described[24,31], WMDW ventilation through the SG is modulated by several physical processes among which the WMDW formation events in the Gulf of Lions and the intensification of the Western Alboran Gyre (WAG, red arrow in Fig. S1) in the Alboran Sea are probably the most relevant. The WAG provides additional energy necessary to uplift deep waters from the Alboran Sea, facilitating the arrival of WMDW to the eastern entrance of the SG[31]. On the contrary, the absence or the relaxation of the WAG propitiates a major drainage of the LIW. Both processes can be traced in the monitoring station by gradual drops of potential temperature to values below 13.1°C[24]. During the monitoring period, such Θ fall was clearly registered in January 2013 (Fig. 1a), which was accompanied by a concomitant rise in the WMDW fraction and a decrease in the LIW fraction (Fig. 2a,b). A similar pattern was also observed in February 2014 and February 2015 (Figs 1a and 2a,b). In a previous study that also used potential temperature as the parameter to trace water masses in the area[24], WDMW formation events left a noticeable signature around March. Following the procedure described by these authors, the densest sample recorded in every semidiurnal tidal cycle was then extracted from our database to obtain

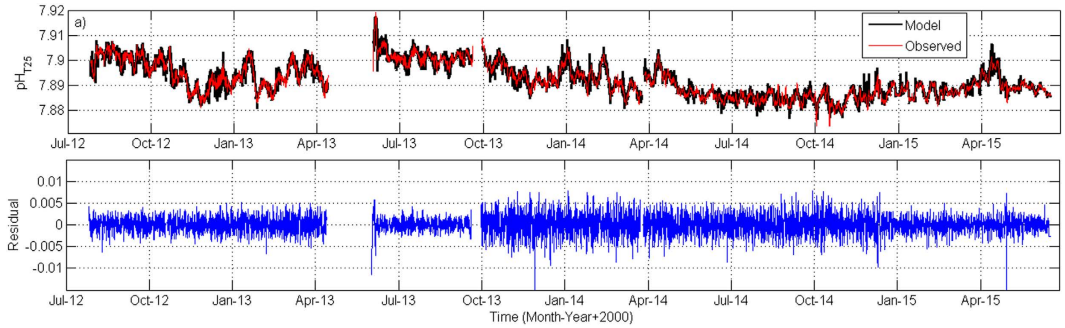

Figure 3. (**a**) pH_{T25} obtained with the SAMI device averaged to 84 h (red line) and modelled pH_{T25} (black line), (**b**) Residuals between observed values and modelled outputs.

a new subseries with semidiurnal sampling interval (not shown). In this new subseries, the major Θ diminutions were found to commence by the middle of January 2013 and beginning of February 2014, with a gradual drop from ~13.2°C to values below 13.05 °C taking place in around 9 days in year 2013 and 13 days in 2014. The original temperature was recovered a month later approximately, a fact that may be partially attributed to the relaxation of the WAG.

Modelled data. As shown in Fig. 3a, the pH data modelled by a MLR (MultiLinear Regression, see *SI text*) faithfully reproduced *in situ* values (averaged to 84 h for comparison), and discrepancies between observational data and modelled outputs were in the order of ±0.005 pH units. Averaging such discrepancies to a 6 h period (Fig. 3b), residuals followed the tidal cycle pattern, thereby confirming that tidal variability was excluded in our estimations. However, higher residuals could still be detected during some periods. For instance, a sharp decline was evident in June 2013 (Fig. 3b), when pH data were recalculated from A_T and pCO_2 measurements. This signal coincides with a rise in the pH_{T25} values (Fig. 1c) and it could be then attributed to the SAMI-CO_2 instrument stabilization time. A second period of higher residual values was observed in October 2013 lasting until April 2014 (Fig. 3b), which may be attributable in this case to the change in the SAMI-pH sampling interval from hourly to bi-hourly. pCO_2 data measured uninterruptedly in the MOW from June 2013 to December 2014 by a SAMI-CO_2 device were also modelled by the MLR (see Fig. S3), with very low residuals being obtained, which supports the model robustness.

As each water mass is characterized by a distinctive salinity and potential temperature, pH can also act as a tracer to define water masses. The OMP and MLR analysis allowed determining that LIW and WDMW in the SG were characterized by average pH_{T25} and standard error values of 7.8897 ± 0.0003 and 7.9077 ± 0.0004, respectively (see Fig. 4). Those values faithfully correspond to recently reported measures[18] equal to ~7.89 for the LIW in the SG and 7.9–7.91 for the WMDW in the Western Mediterranean basin. Differences in pH values betwen both water masses can be explained on the basis of the transit times from their respective formation sites to the SG; the LIW takes around 8 years to complete the distance from the Levantine basin (LB, Fig. S1) to the Strait of Sicile (SS, Fig. S1)[32]. An active remineralization of organic matter can take place during such period, which implies the rise of dissolved inorganic carbon concentration, the decrease of dissolved oxygen and the consequent pH decrease[16,18]. In contrast, the WMDW takes roughly 1.8 years to travel from the Gulf of Lions to the Alboran Sea (GL and AS respectively in Fig. S1), a much shorter transit time[33]. Although the ventilation time of LIW and WMDW is an issue that has not been solved yet and there are still large discrepancies regarding the age of each water mass[34–37], estimated ages are around 80–120 ± 20 yr and 20–40 ± 40 yr for the bottom waters of the eastern and western basins, respectively, when they arrive at the SG[35]. Therefore, considering the circulation pattern in the MS[38] and regardless of a particular transit time or age for each water mass, when they both arrive at the SG the WMDW is much younger than the LIW formed in the distant Levantine Basin (LB, Fig. S1). Accordingly, the LIW is more stable than the WMDW from a biogechemical point of view, as the former lost contact with the atmosphere a longer ago. Therefore, in the SG, the WMDW,which has been exposed to the atmosphere more recently, exhibits higher pH values than the eastern-originated LIW (Fig. 4). This is confirmed when the monthly variability of pH in both water masses is analysed (see Fig. S2). Although a little seasonality can be detected, over the summer months, the two water masses showed stable pH values whereas winter conditions resulted in the highest pH variability, which was especially remarkable in February. During this month, pH in the WMDW presented noticeable oscillations, ranging from 7.7789 to 8.0003 whereas the pH of the LIW varied slightly, with values changing from 7.8195 to 7.9634. This seasonal variability could be again attributed to the ventilation pattern of the WMDW. A previous work[25] demostrated that a lag of few weeks can be found between the events of WMDW fomation in winter in the Gulf of Lions and the detection of cold pulses of old WMDW at the

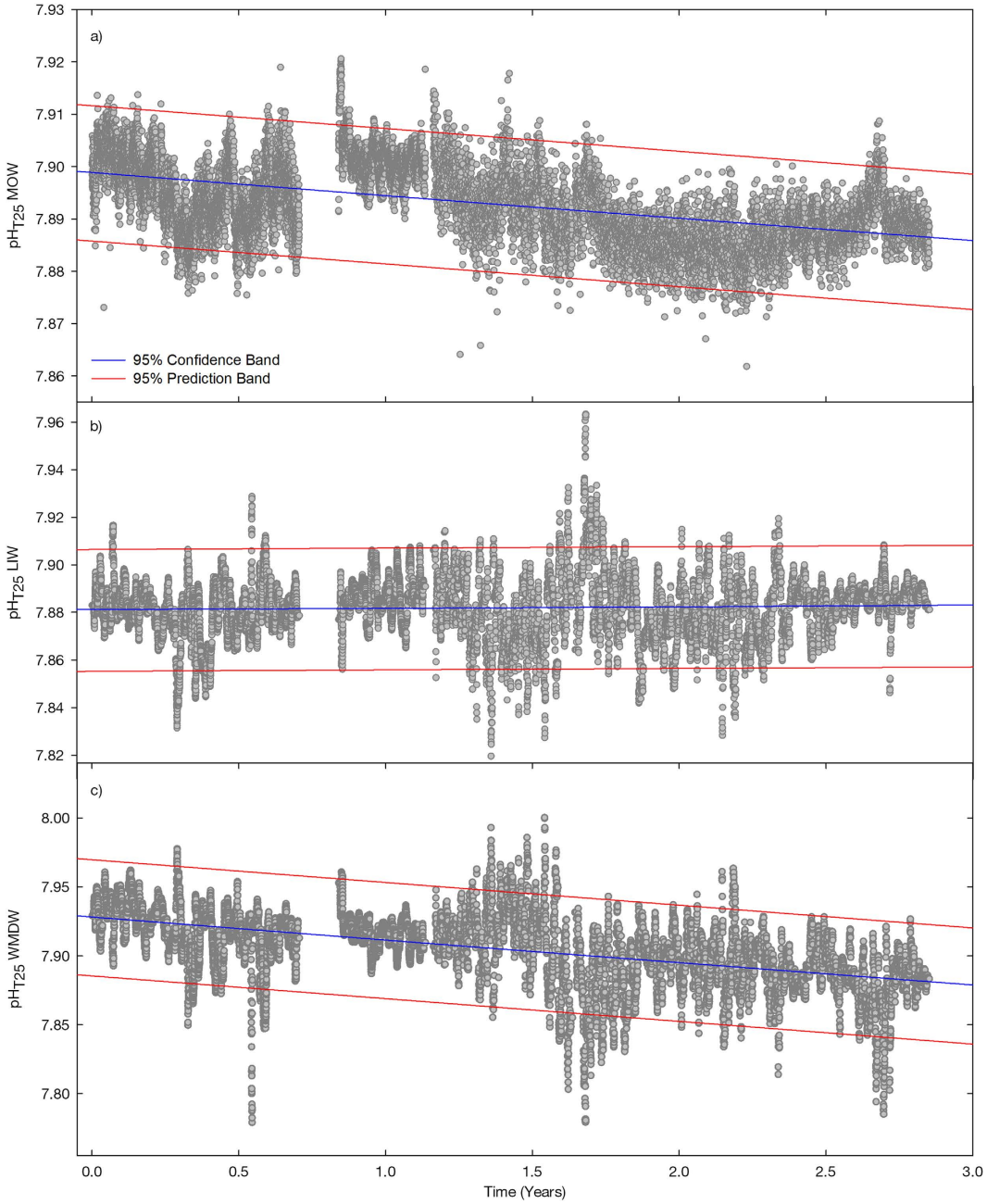

Figure 4. Linear fitting of pH with time (see SI *text*) of the MOW and its forming water masses during the monitoring period: **(a)** MOW, **(b)** LIW and **(c)** WMDW. Blue and red lines represent the 95% confidence and prediction bands, respectively. Equations are shown in the SI *text*. Note the different scales for "y" axes in figures (**a–c**).

monitoring site in Espartel Sill. Renovation of the old resident WMDW in the SG depends on the volume of water formed during winter by deep convection in the Gulf of Lions and the intensification of the WAG that subsequently uplifts the ancient WMDW at the SG. During our study period, the appearance of colder (and older) WDMW pulses in February 2013, 2014 and 2015 (Figs 1a and 2b) possibly resulted in the lowest pH values detected in the WMDW during the months of February (see Fig. S2b), as the older WMDW residing in the eastern side of the Strait will be characterized by lower pH values, due to the active remineralization processes occurring in the Alboran basin[39].

Trends of pH decrease in Mediterranean waters. The pH data series clearly depicted a negative trend (Fig. 1) although the data gap after the first period (April-June 2013) seems to visually break the tendency. From June 2013 onwards, the decreasing trend was even clearer. Taking into account the

whole period, a pH-time linear regression was calculated (see *SI text* for calculation details) and plotted in Fig. 4. The regression statistics were significant and resulted in a ΔpH of -0.0044 units per year in the MOW. This rate of pH decline is of the same order of magnitude than acidification rates reported by sustained observations of different carbon system parameters collected in several oceanic seasurface time series[21], although it is two or three fold higher than those (depending on the site). Nevertheless, it still falls within the range of pH change in Mediterranean deep waters estimated recently through a modelling approach (-0.005 to -0.06 pH units[13]).

The consistency of our pH decreasing pattern is supported by the complementary pCO_2 measurements taken in the SG at the same sampling frequency. When the ΔpCO_2 in the MOW obtained during the monitoring period is calculated, an increase in pCO_2 of 5.1 μatm y^{-1} is obtained (see *SI text* and Fig. S4 for calculation details). This CO_2 rise is coherent with (and matches) the rate of pH decline observed in the MOW.

Performing a separate analysis for each of the two main water masses forming the MOW, annual decline rates of -0.0006 and -0.0165 pH units per year are calculated for the LIW and WMDW, respectively (Fig. 4b,c). The regression descriptors were statistically significant (see *SI text*). These pH changes correspond to pCO_2 variations of -0.6 and 18.5 μatm in each water mass respectively (see Fig. S4), according to the CO_2 data in the SG.

The low ΔpH_{LIW} may be well attributable to its age (in the order of 100 years upon arrival at the SG) and stability, as this intermediate water mass has not been affected by the present atmopheric CO_2 concentrations. On the other hand, the more recently produced WMDW showed a considerable pH decreasing trend and a noticeable pCO_2 rise. As previously noted, this may be a consequence of several processes. First, the impact of higher atmospheric CO_2 concentration this water mass was exposed to when formed, secondly, the faster penetration of CO_2 in the water column brought about by the high alkalinity of this water mass[40] and finally the sinking of labile and easily oxidizable organic matter facilitated by the formation events. Also, both LIW and WMDW reflect the gradient of trophic conditions from the Western to the Eastern Mediterranean basin. With a eastward decreasing gradient pattern of primary productivity[41], the Alboran Sea represents one of the most productive Mediterranean areas[41] involving a greater deep degradation potential of organic inputs coming from the photic zone[42]. Therefore, the WMDW, support high rates of organic carbon degradation[42,43] and subsequently an increase on the CO_2 content while residing in the deep Alboran Sea.

Observations gathered in other time series have shown that ocean regions characterized by high rates of increase in pCO_2 (Irminger Sea and CARIACO, for instance) depict the highest rates of decrease in surface seawater pH (around -0.0025 pH units y^{-1})[21].

Even though the time period of observations used in our work (roughly 3 years) can be considered relatively short to asses long term changes in the pH of the Mediterranean Sea, it still provides a reasonable wealth of data with sufficient sensitivity and accuracy to establish seasonal and interannual pH variations in the water masses of the Mediterranean Sea that reflect changes in both the natural carbon cycle and anthropogenic perturbation. It is worthy to point out that, in addition to the uptake of anthropogenic CO_2 from the atmosphere, the Mediterranean basin receives continuously a considerable amount of anthropogenic carbon from the North Atlantic Ocean through the SG[20]. Monitoring the magnitude of the resulting pH decline in the basin requires sustained high-accuracy observations. The data presented here may well serve as a base line to assess sensitiviy and evolution of the Mediterranean waters to the impact of increasing CO_2 emmissions.

Methods

pH measurements shown in this study were collected from August 2012 to June 2015 at the GIFT time series in the Strait of Gibraltar (see *SI text* for mooring line details, Fig. S1). Water masses fractions within the MOW were obtained by an Optimum MultiParameter (OMP) analysis and modelled pH was constructed by performing a Multiple Linear Regression (MLR) least square fitting. In order to smooth out the short-scale variability and turbulence originated in the supercritical-to-subcritical flow transitions[44] as well as the fluctuations associated with the tidally-generated short internal waves in the SG, which result mostly in the rapid mixing between water masses, data were averaged in periods of 84 hours (half week), as our work was meant to focus on long-term variability related to basin scale processes, which is relevant for OA signals. Details regarding the CO_2 system calculations, data sets used and the statistical treatment may be found in SI (see *SI text*).

References

1. Cubasch, U. *et al.* in *Climate Change 2013: The Physical Science Basis. Contribution of Working Group I to the Fifth Assessment Report of the Intergovernmental Panel on Climate Change* (eds T. F. Stocker *et al.*) Ch. 1, 119–158 (Cambridge University Press, 2013).
2. Le Quéré, C. *et al.* Global carbon budget 2013. *Earth System Science Data* **6,** 235–263, doi: 10.5194/essd-6-235-2014 (2014).
3. Le Quéré, C., Takahashi, T., Buitenhuis, E. T., Rödenbeck, C. & Sutherland, S. C. Impact of climate change and variability on the global oceanic sink of CO_2. *Glob. Biogeochem. Cycle* **24,** GB4007, doi: 10.1029/2009GB003599 (2010).
4. Gattuso, J.-P., Mach, K. & Morgan, G. Ocean acidification and its impacts: an expert survey. *Climatic Change* **117,** 725–738, doi: 10.1007/s10584-012-0591-5 (2013).
5. Doney, S. C., Fabry, V. J., Feely, R. A. & Kleypas, J. A. Ocean acidification: the other CO_2 problem. *Annual Review of Marine Science* **1,** 169–192, doi: 10.1146/annurev.marine.010908.163834 (2009).

6. Fabry, V. J., Seibel, B. A., Feely, R. A. & Orr, J. C. Impacts of ocean acidification on marine fauna and ecosystem processes. *ICES Journal of Marine Science: Journal du Conseil* **65,** 414–432, doi: 10.1093/icesjms/fsn048 (2008).
7. Orr, J. C. *et al.* Anthropogenic ocean acidification over the twenty-first century and its impact on calcifying organisms. *Nature* **437,** 681–686, doi: 10.1038/nature04095 (2005).
8. Feely, R. A., Doney, S. C. & Cooley, S. R. Ocean acidification: present conditions and future changes in a high-CO_2 world. *Oceanography* **22,** 36–47 (2009).
9. Ríos, A. F. *et al.* Decadal acidification in the water masses of the Atlantic Ocean. *Proceedings of the National Academy of Sciences*, doi: 10.1073/pnas.1504613112 (2015).
10. Bramanti, L. *et al.* Detrimental effects of ocean acidification on the economically important Mediterranean red coral (Corallium rubrum). *Global Change Biology* **19,** 1897–1908, doi: 10.1111/gcb.12171 (2013).
11. Calvo, E. *et al.* Effects of climate change on Mediterranean marine ecosystems: the case of the Catalan Sea. *Climate Research* **50,** 1–29 (2012).
12. Hassoun, A. E. R. *et al.* Acidification of the Mediterranean Sea from anthropogenic carbon penetration. *Deep Sea Research Part I: Oceanographic Research Papers* **102,** 1–15 (2015).
13. Palmiéri, J. *et al.* Simulated anthropogenic CO_2 storage and acidification of the Mediterranean Sea. *Biogeosciences* **12,** 781–802, doi: 10.5194/bg-12-781-2015 (2015).
14. Touratier, F. & Goyet, C. Impact of the eastern mediterranean transient on the distribution of anthropogenic CO_2 and first estimate of acidification for the Mediterranean Sea. *Deep Sea Research Part I: Oceanographic Research Papers* **58,** 1–15 (2011).
15. Touratier, F. & Goyet, C. Decadal evolution of anthropogenic CO_2 in the northwestern Mediterranean Sea from the mid-1990s to the mid-2000s. *Deep-Sea Research Part I-Oceanographic Research Papers* **56,** 1708–1716, doi: 10.1016/j.dsr.2009.05.015 (2009).
16. Rivaro, P., Messa, R., Massolo, S. & Frache, R. Distributions of carbonate properties along the water column in the Mediterranean Sea: Spatial and temporal variations. *Marine Chemistry* **121,** 236–245 (2010).
17. Touratier, F. *et al.* Distributions of the carbonate system properties, anthropogenic CO_2, and acidification during the 2008 BOUM cruise (Mediterranean Sea). *Biogeosciences Discussions* **9,** 2709–2753 (2012).
18. Álvarez, M. *et al.* The CO_2 system in the Mediterranean Sea: a basin wide perspective. *Ocean Sci.* **10,** 69–92, doi: 10.5194/os-10-69-2014 (2014).
19. Schneider, A., Tanhua, T., Körtzinger, A. & Wallace, D. W. High anthropogenic carbon content in the eastern Mediterranean. *Journal of Geophysical Research: Oceans (1978–2012)* **115,** C12050, doi: 10.1029/2010JC006171 (2010).
20. Huertas, I. E. *et al.* Anthropogenic and natural CO_2 exchange through the Strait of Gibraltar. *Biogeosciences* **6,** 647–662 (2009).
21. Bates, N. R. *et al.* A time-series view of changing ocean chemistry due to ocean uptake of anthropogenic CO_2 and ocean acidification. *Oceanography* **27,** 126–141, doi: 10.5670/oceanog.2014.16 (2014).
22. Millot, C. Circulation in the western Mediterranean Sea. *Journal of Marine Systems* **20,** 423–442 (1999).
23. Millot, C. & Taupier-Letage, I. in *The Mediterranean Sea* 29–66 (Springer, 2005).
24. García-Lafuente, J. *et al.* Interannual variability of the Mediterranean outflow observed in Espartel sill, western Strait of Gibraltar. *Journal of Geophysical Research: Oceans (1978–2012)* **114,** C10018, doi: 10.1029/2009JC005496 (2009).
25. García Lafuente, J., Sánchez Román, A., Díaz del Río, G., Sannino, G. & Sánchez Garrido, J. Recent observations of seasonal variability of the mediterranean outflow in the Strait of Gibraltar. *Journal of Geophysical Research: Oceans (1978–2012)* **112,** C10005, doi: 10.1029/2006JC003992 (2007).
26. Flecha, S. *et al.* Anthropogenic carbon inventory in the Gulf of Cádiz. *Journal of Marine Systems* **92,** 67–75, doi: 10.1016/j.jmarsys.2011.10.010 (2012).
27. Huertas, I. E. *et al.* Atlantic forcing of the Mediterranean oligotrophy. *Global Biogeochem. Cycles* **26,** GB2022, doi: 10.1029/2011gb004167 (2012).
28. Sánchez-Román, A., Sannino, G., García-Lafuente, J., Carillo, A. & Criado-Aldeanueva, F. Transport estimates at the western section of the Strait of Gibraltar: A combined experimental and numerical modeling study. *Journal of Geophysical Research: Oceans* **114,** C06002, doi: 10.1029/2008JC005023 (2009).
29. García-Lafuente, J., Sánchez-Román, A., Naranjo, C. & Sánchez-Garrido, J. C. The very first transformation of the Mediterranean outflow in the Strait of Gibraltar. *Journal of Geophysical Research: Oceans (1978–2012)*, C07010, **116,** doi: 10.1029/2011JC006967 (2011).
30. Tomczak, M. & Large, D. G. B. Optimum multiparameter analysis of mixing in the thermocline of the eastern Indian Ocean. *Journal of Geophysical Research: Oceans* **94,** 16141–16149, doi: 10.1029/JC094iC11p16141 (1989).
31. Naranjo, C., García Lafuente, J., Sánchez Garrido, J. C., Sánchez Román, A. & Delgado Cabello, J. The western alboran gyre helps ventilate the western mediterranean deep water through Gibraltar. *Deep Sea Research Part I: Oceanographic Research Papers* **63,** 157–163 (2012).
32. Roether, W., Klein, B., Beitzel, V. & Manca, B. B. Property distributions and transient-tracer ages in Levantine Intermediate Water in the Eastern Mediterranean. *Journal of Marine Systems* **18,** 71–87 (1998).
33. Schmidt, S. & Reyss, J.-L. Radium as internal tracer of Mediterranean Outflow Water. *Journal of Geophysical Research: Oceans* **101,** 3589–3596, doi: 10.1029/95JC03308 (1996).
34. Andrie, C. & Merlivat, L. Tritium in the western Mediterranean Sea during 1981 Phycemed cruise. *Deep Sea Research Part A. Oceanographic Research Papers* **35,** 247–267, doi: 10.1016/0198-0149(88)90039-8 (1988).
35. Stratford, K., Williams, R. G. & Drakopoulos, P. G. Estimating climatological age from a model-derived oxygen–age relationship in the Mediterranean. *Journal of Marine Systems* **18,** 215–226, doi: 10.1016/S0924-7963(98)00013-X (1998).
36. Stratford, K. & Williams, R. G. A tracer study of the formation, dispersal, and renewal of Levantine Intermediate Water. *Journal of Geophysical Research: Oceans* **102,** 12539–12549, doi: 10.1029/97JC00019 (1997).
37. Rhein, M. Deep water formation in the western Mediterranean. *Journal of Geophysical Research: Oceans* **100,** 6943–6959, doi: 10.1029/94JC03198 (1995).
38. Millot, C. Another description of the Mediterranean Sea outflow. *Progress in Oceanography* **82,** 101–124 (2009).
39. Minas, H. J., Coste, B., Le Corre, P., Minas, M. & Raimbault, P. Biological and geochemical signatures associated with the water circulation through the Strait of Gibraltar and in the western Alboran Sea. *Journal of Geophysical Research: Oceans* **96,** 8755–8771, doi: 10.1029/91JC00360 (1991).
40. Copin-Montégut, C. & Bégovic, M. Distributions of carbonate properties and oxygen along the water column (0–2000m) in the central part of the NW Mediterranean Sea (Dyfamed site): influence of winter vertical mixing on air–sea CO_2 and O_2 exchanges. *Deep Sea Research Part II: Topical Studies in Oceanography* **49,** 2049–2066 (2002).
41. Skliris, N. & Beckers, J.-M. Modelling the Gibraltar Strait/Western Alboran Sea ecohydrodynamics. *Ocean Dynamics* **59,** 489–508 (2009).
42. Sanchez-Vidal, A., Calafat, A., Canals, M., Frigola, J. & Fabres, J. Particle fluxes and organic carbon balance across the Eastern Alboran Sea (SW Mediterranean Sea). *Continental Shelf Research* **25,** 609–628, doi: 10.1016/j.csr.2004.11.004 (2005).
43. Luna, G. M. *et al.* The dark portion of the Mediterranean Sea is a bioreactor of organic matter cycling. *Glob. Biogeochem. Cycle* **26,** n/a-n/a, doi: 10.1029/2011GB004168 (2012).

44. Sánchez-Garrido, J. C., Sannino, G., Liberti, L., García Lafuente, J. & Pratt, L. Numerical modeling of three-dimensional stratified tidal flow over Camarinal Sill, Strait of Gibraltar. *Journal of Geophysical Research: Oceans* **116,** C12026, doi: 10.1029/2011JC007093 (2011).

Acknowledgements

The cooperation of the captains and crews of the research vessels "Cornide de Saavedra", "Angeles Alvariño", "Ramon Margalef" and "Sarmiento de Gamboa" is greatly appreciated. We also thank María Ferrer, Antonio Moreno, David Roque and Cristina Naranjo for assistance during mooring operations. Funding for this work was provided by the European Commission through the projects CARBOCHANGE (FP7-264879), and PERSEUS (FP7-287600) and by the Spanish Ministry of Economy and Competitiveness (CTM2010-21229). SF was supported by a JAE PREDOCTORAL scholarship, part-funded by the European Commission (European Social Fund, ESF2007-2013) and the Spanish Ministry for Economy and Competitiveness.

Author Contributions

S.F. and I.E.H. wrote the manuscript text and supporting information. S.F. prepared all the figures. S.F., F.F.P. and S.S. analized the data. I.E.H. and J.G.-L. have contributed to the conception and design of the study. F.F.P., J.G.-L. and A.F.R. have contributed in the results discussion. All authors reviewed the manuscript and supporting information. S.F. and I.E.H. made equal contributions.

Additional Information

Supplementary information accompanies this paper at http://www.nature.com/srep

Competing financial interests: The authors declare no competing financial interests.

How to cite this article: Flecha, S. *et al.* Trends of pH decrease in the Mediterranean Sea through high frequency observational data: indication of ocean acidification in the basin. *Sci. Rep.* **5**, 16770; doi: 10.1038/srep16770 (2015).

Supplementary Information (SI) of:

Trends of pH decrease in the Mediterranean Sea through high frequency observational data: indication of ocean acidification in the basin

Susana Flecha[1*], Fiz F. Pérez[2], Jesús García-Lafuente[3], Simone Sammartino[3], Aida. F. Ríos[2] and I. Emma Huertas[1*]

SI Text

Data recording. The mooring line deployed in the Espartel Sill (ES) consists of an uplooking Acoustic Doppler Current Profiler (ADCP) (Teledyne RD Instruments, Inc.), a currentmeter Nortek Aquadopp (Nortek AS), a CT (Conductivity Temperature) SBE 37 probe (Sea-Bird Electronics, Inc.), and SAMI-pH and SAMI-CO_2 Submersible Autonomous Moored Instruments (Sunburst Sensors, LLC.). CT, SAMI-pH and SAMI-CO_2 were placed around 13 m above the sea bottom (360 m depth) (Fig. S1). Precision and accuracy of measurements were < 0.001 and ± 0.003 pH units and < 1 ppm and ± 3 ppm for SAMI pH and pCO_2 instruments, respectively. Calibrations of instruments were performed by the manufacturer companies for the SAMI-CO_2 and for two CT's used periodically. SAMI-CO_2 used was acquired and calibrated previously to the deployment. CT's drifts obtained of +0.0001 and -0.00006 ºC/year and 0.0001 and 0.0000 PSU/month for temperature and salinity, respectively, were applied to the data. SAMI-pH data were validated with periodically laboratory calibrations by using Certified Reference Material (CRM supplied by Prof. Andrew Dickson, Scripps Institution of Oceanography, La Jolla, CA, USA) and a Shimadzu UV-2401PC spectrophotometer containing a 25 °C-thermostated cells holder

following a spectrophotometric method[1]. In addition, the drift obtained for the SAMI-pH from the manufacturer of 0.001pH over 6 months was applied to the obtained data.

pH data can be divided in 3 periods: 1) August 2012-April 2013, 2) June 2013-September 2013 and 3) October 2013-June 2015. During the first and third periods data were collected with the SAMI-pH sensor every 60 and 120 minutes, respectively. The sampling interval was changed in order to extend the batteries life and to ensure data acquisition during a longer period because, occasionally, the line cannot be recovered when planned due to adverse meteorological conditions in the Strait. In fact, data were missed during the second period because the batteries ran out before the devices could be lifted. To fill the data gap occurred in summer 2013, pH data were calculated from: the pCO_2 data obtained with the SAMI-CO_2 (which was operative during such period as the batteries had a longer life time), the Total Alkalinity (A_T)-Salinity relationship reported previously [2] in the area by using the carbonic acid apparent dissociation constants more appropriate for the SG waters [3,4].

CT data were recorded every 30 minutes and practical salinity (TEOS-10), salinity hereinafter, and potential temperature (Θ) were used afterwards to compute pH at *in situ* salinity and resolve the water masses structure within the MOW by an Optimum MultiParameter Analysis (OMP). Temperature and salinity chosen for OMP water masses characterization end members were 13.22, 12.8, 15º C and 38.56, 38.45, 36.8 for LIW, WMDW and AW respectively[5].

pH modeling, Trend Determinations and Statistics. pH was modeled through the classical MLR scheme that allows establishing the relationship between a response variable (pH) and some predictors (in this case the fraction of the three water masses that can be found in the Strait, fAW, fWMDW and fLIW) by using a linear combination of the predictors. The result of our data fitting was:

pH±0.0073=7.8577±0.0018*fAW+7.9077±0.0004*fWMDW+7.8897±0.0003*fLIW (R^2=0.999; n=15937),

where the predicted variable, the obtained coefficients and the standard error are indicated. Comparable results were obtained with pCO_2 as the predicted variable (Fig. S3).

Trends in pH and pCO_2 were determined by ordinary linear regression and standard errors and 95% confidence intervals were calculated for the slopes of the regressions. In the case of the MOW, pH linear fitting with time is represented by the equation:

$pH_{MOW} = -0.0044 \pm 6.2094 * 10^{-5}\ t + 7.8987 \pm 9.1824 * 10^{-5}$ ($R^2 = 0.2362$; $p<0.01$; $n=15937$),

whereas the results of the fitting for the WMDW and LIW were given by the following expressions:

$$pH_{WMDW} = -0.0165 \pm 0.0002\ t + 7.9276 \pm 0.0003\ (R^2 = 0.2946;\ p<0.01;\ n=15937),$$

$$pH_{LIW} = -0.0006 \pm 0.0001\ t + 7.8822 \pm 0.0002\ (R^2 = 0.0011;\ p<0.01;\ n=15937),$$

where t represents time (years) starting from August 8th , 2012 to June 15th ,2015. Standard errors are also shown.

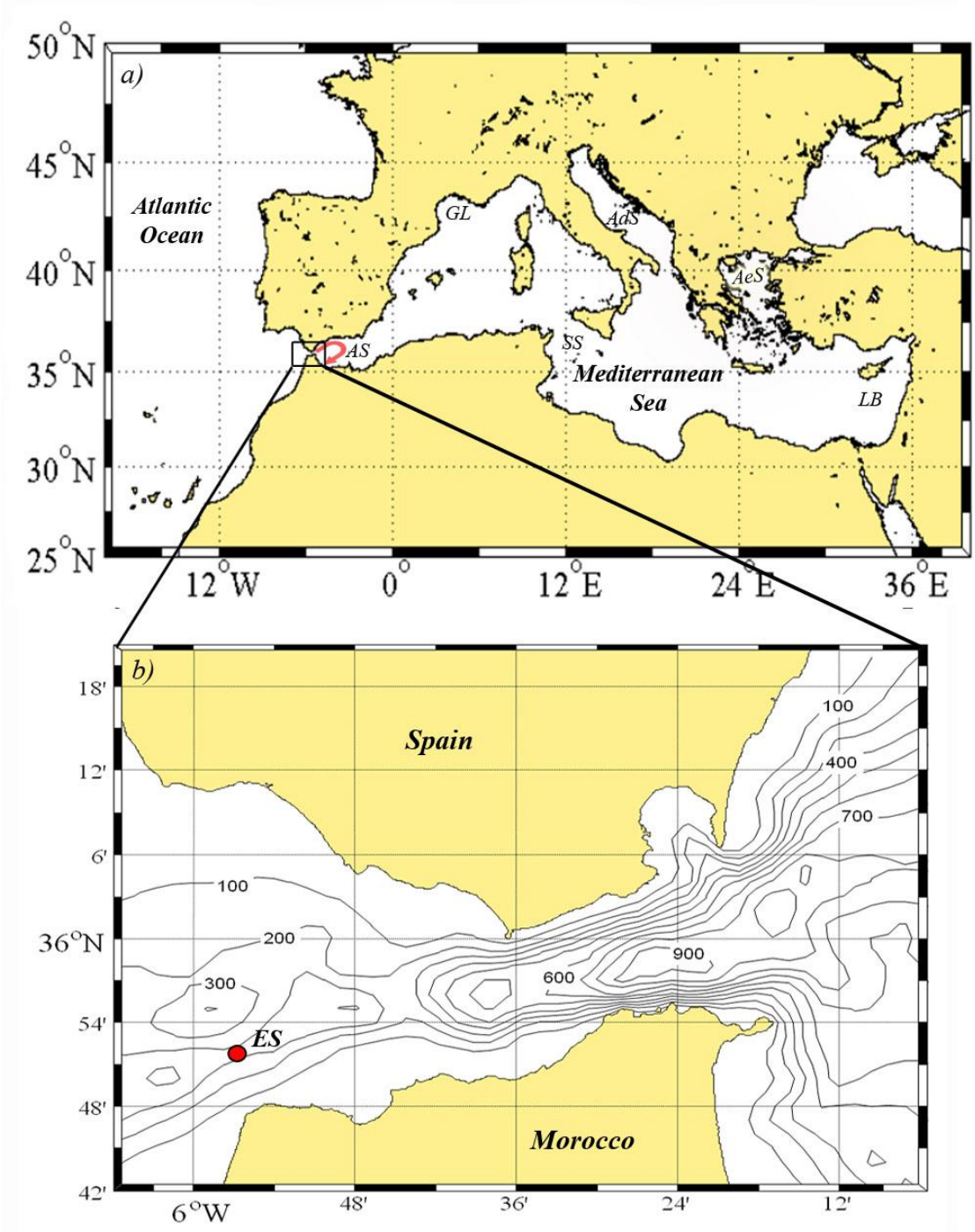

Fig. S1: a) Map of the Mediterranean Sea, detailing the location of different sub-basins: Alboran Sea (AS), Gulf of Lions (GL) Adriatic Sea (AdS), Aegean Sea (AeS), Levantine Basin (LB) and the Strait of Sicily (SS), b) map of the Strait of Gibraltar showing the mooring line location at the Espartel Sill (ES). Maps were developed with the MATLAB® software by using the M_Map toolbox.

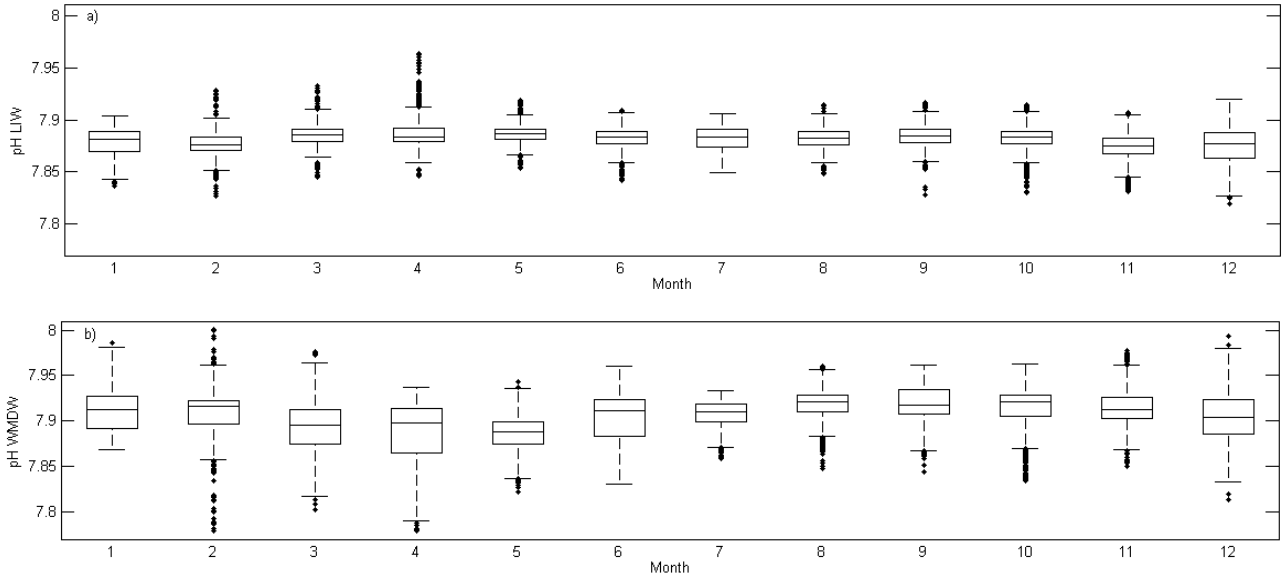

Fig. S2: Monthly pH values of the water masses forming the MOW during the monitoring period: a) LIW and b) WDMW. The tops and bottoms of each "box" are the 25th and 75th percentiles of the samples, respectively. The distances between the tops and bottoms are the interquartile ranges whereas the line in the middle of each box is the sample median. Observations beyond the whisker length are marked as outliers displayed with a black dot.

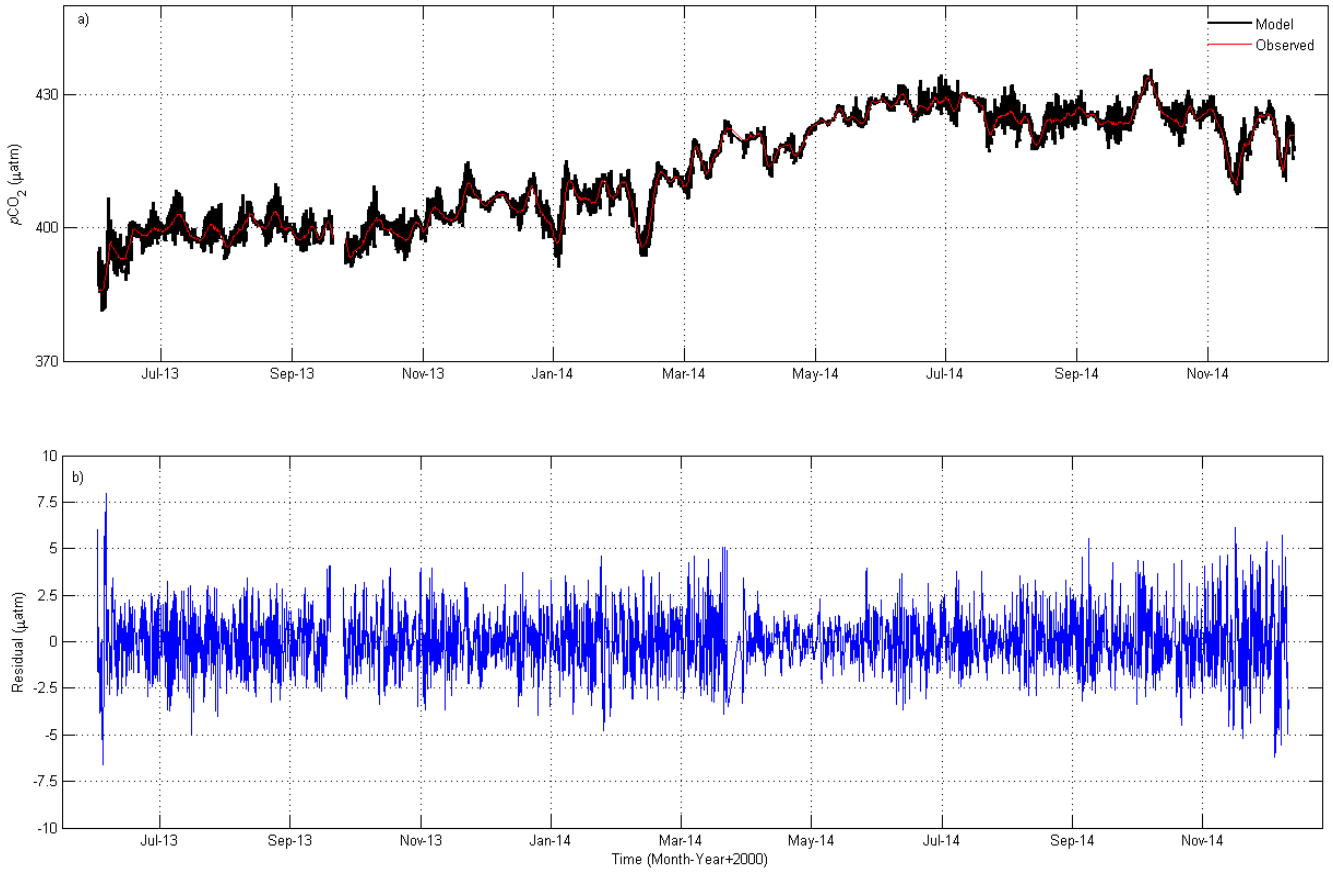

Fig. S3: a) pCO_2 obtained with the SAMI device averaged to 84 h (red line) between June 2013 and November 2014 and modelled pCO_2 (black line), b) Residuals between observed values and modelled outputs.

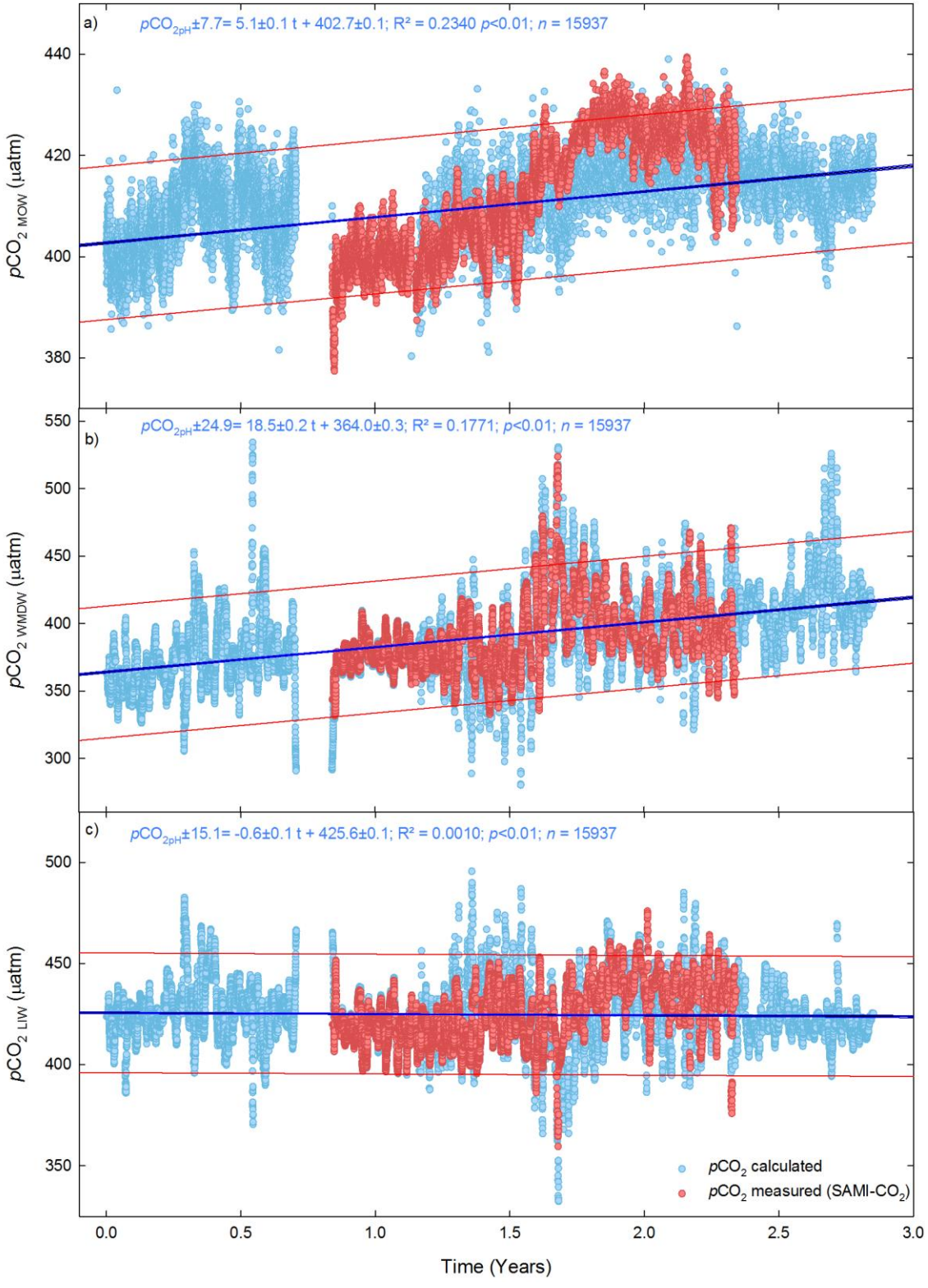

Fig. S4: Linear fitting of pCO_2 with time (see SI *text*) of the MOW and its forming water masses during the monitoring period: a) MOW, b) LIW and c) WMDW. Blue and red lines

represent the 95% confidence and prediction bands, respectively. Note the different scales for "y" axes in figures a, b and c.

References

1. Clayton TD, Byrne RH. Spectrophotometric seawater pH measurements: total hydrogen ion concentration scale calibration of m-cresol purple and at-sea results. *Deep Sea Research Part I: Oceanographic Research Papers* **40**, 2115-2129 (1993).

2. Huertas IE, *et al.* Anthropogenic and natural CO_2 exchange through the Strait of Gibraltar. *Biogeosciences* **6**, 647-662 (2009).

3. Mehrbach C, Culberson CH, Hawley JE, Pytkowicz RM. Measurement of the apparent dissociation constants of carbonic acid in seawater at atmospheric pressure. *Limnology and Oceanography* **18**, 897-907 (1973).

4. Dickson A, Millero F. A comparison of the equilibrium constants for the dissociation of carbonic acid in seawater media. *Deep Sea Research Part A Oceanographic Research Papers* **34**, 1733-1743 (1987).

5. García Lafuente J, Sánchez Román A, Díaz del Río G, Sannino G, Sánchez Garrido J. Recent observations of seasonal variability of the Mediterranean outflow in the Strait of Gibraltar. *Journal of Geophysical Research: Oceans (1978–2012)* **112**, C10005, (2007). doi:10.1029/2006JC003992.